

Identification of Ligand-Binding Regions of P-Glycoprotein by Activated-Pharmacophore Photoaffinity Labeling and Matrix-Assisted Laser Desorption/Ionization–Time-of-Flight Mass Spectrometry

GERHARD F. ECKER, EDINA CSASZAR, STEPHAN KOPP, BRIGITTE PLAGENS, WOLFGANG HOLZER, WOLFGANG ERNST, and PETER CHIBA

Institutes of Medical Chemistry (P.C., S.K.), Pharmaceutical Chemistry (G.E., B.P., W.H.), Applied Microbiology (W.E.), and the Mass Spectrometry Unit (E.C.), University of Vienna, Austria

Received July 26, 2001; accepted November 16, 2001

This article is available online at <http://molpharm.aspetjournals.org>

ABSTRACT

Energy dependent efflux pumps confer resistance to anticancer, antimicrobial, and antiparasitic drugs. P-glycoprotein (Pgp, ABCB1) mediates resistance to a broad spectrum of antitumor drugs. Compounds that themselves are nontoxic to cells have been shown to act as inhibitors of Pgp. The mechanism of binding and transport of low-molecular-mass ligands by Pgp is still incompletely understood. This study introduces a series of propafenone-related photoaffinity ligands, which combine high specificity and selectivity for Pgp with high labeling efficiency. Molecules are intrinsically photoactivatable in the arylcarbonyl group, which represents a pharmacophoric substructure for this group of ligand molecules. A detailed study of the structure-activity relationship for this type of photoligand is presented. In subsequent experiments, these ligands were used to characterize the drug-binding domain of propafenone-type analogs. Ma-

trix-assisted laser desorption/ionization—time-of-flight (MALDI-TOF) mass spectrometry shows that propafenone-type ligands preferentially label fragments assigned to putative transmembrane segments 3, 5, 6, 8, 10, 11, and 12. Labeled fragments are also identified in a highly charged region of 15 amino acids in the second cytoplasmic loop. This region corresponds to the so-called EAA-like motif, which has been proposed to play a role in the interaction between transmembrane domain and nucleotide binding domain of peroxisomal ATP-binding cassette transporters. In addition, a region in cytoplasmic loop 3 and between TM12 and the N terminus of the Walker A sequence of NBD2 are labeled by the ligands. Therefore, a number of confined protein regions contribute to the drug-binding domain of propafenone-type analogs.

Expression of drug-efflux pumps is one important mechanism for target cells to protect themselves from the lethal action of therapeutically administered drugs. During the past decade, a number of efflux systems in bacteria, fungi, parasites, and mammalian cells were identified. A common property of these efflux pump systems, many of which share a high degree of sequence homology, is broad substrate specificity. The phenotype arising as a consequence of the expression of these efflux pumps has therefore been termed multidrug resistance (MDR). Because advanced drug design paved the way for the circumvention of a number of drug-specific resistance mechanisms, this type of broad-spectrum resistance is also increasingly observed in a clinical setting. The most extensively studied drug transporter is P-glycoprotein

(Pgp). Pgp is a 170-kDa protein of human origin that is constitutively expressed in a variety of human tissues (Gottesman and Pastan, 1993). Overexpression is observed in resistant human tumors of different origin. P-glycoprotein is the functional ortholog of microbial ABC transporters. These include LmrA, an efflux transporter conferring multidrug resistance in *Lactococcus lactis* (van Veen et al., 1996), the yeast transporters snq2p (Servos et al., 1993) and pdr5p (Balzi et al., 1994; Bissinger and Kuchler, 1994) and the *Candida albicans* drug resistance proteins cdr1p (Prasad et al., 1995) and cdr2p (Sanglard et al. 1997).

One concept for the circumvention of MDR is the simultaneous administration of cytotoxic drugs and inhibitors of toxin efflux pumps. These modulators of multiresistance are of interest to the pharmacologist because they are able to reverse MDR in tumor cells (reviewed in Krishna and Mayer,

This work was supported by a grant from the Austrian Science Fund (FWF) (Grant 13851) and the Austrian National Bank (Grant 8525).

ABBREVIATIONS: MDR, multidrug resistance; Pgp, P-glycoprotein; ABC, ATP-binding cassette; QSAR, quantitative structure activity relationship; MS, mass spectrometry; PM, plasma membrane; CHCA, α -cyano-4-hydroxycinnamic acid; MALDI-TOF, matrix-assisted laser desorption/ionization–time-of-flight; TFA, trifluoroacetic acid; PA, propafenone analog; CL, cytoplasmic loop; ECL, extracytoplasmic loop; AA, amino acid; TM, transmembrane segment; NBD, nucleotide binding domain.

2000) and microbial systems (Lomovskaya and Watkins, 2001) in vitro.

A characterization of the interaction of toxin efflux pumps with low-molecular-mass inhibitors has been pursued by photoaffinity labeling (for comprehensive reviews on the subject, see Beck and Qian, 1992; Dey et al., 1998; Greenberger, 1998; Safa, 1998), site-directed mutagenesis (Loo and Clarke, 1998, 2000, 2001a,b), ligand-based design (see the recent review by Wiese and Pajeva, 2001, and references therein), and Pgp-ATPase activity measurements (reviewed in Senior et al., 1998).

Cysteine scanning and site-directed mutagenesis identified amino acid residues in transmembrane segments, which are likely to be involved in drug binding (Ma et al., 1997; Dey et al., 1999; Loo and Clarke, 2000, 2001b). Electron cryo-microscopy of two-dimensional crystals has led to structural resolution of hamster Pgp at approximately 10 Å (Rosenberg et al., 2001). Despite this progress, the interaction of ligand molecules with Pgp is still inadequately defined on a molecular basis. We thus pursued an approach combining ligand-based design in conjunction with quantitative structure activity relationship (QSAR) studies to characterize the interaction of low-molecular-mass ligands with Pgp in greater detail.

On the basis of studies conducted on a compound library of substances that are structurally related to propafenone, common structural and physicochemical parameters of this class of inhibitors have been defined and pharmacophoric substructures have been identified (Chiba et al., 1996; Ecker et al., 1996, 1999).

Photoaffinity labeling represents one possible experimental strategy to characterize those regions of the protein molecule in which an interaction with low-molecular-mass ligands takes place. Similar to certain steroids, propafenone and its analogs are intrinsically photoactivatable, whereby activation takes place in the arylcarbonyl substructure. We previously identified the carbonyl group as a pharmacophore with respect to Pgp (Chiba et al., 1996). This group acts as a hydrogen bond acceptor, which is likely to interact with a hydrogen bond donor group in the protein (Ecker et al., 1999).

Formation of the biradical species is favoured, when the carbonyl group is part of a benzophenone substructure. Therefore, a series of propafenone-analogous molecules containing a benzophenone substructure were synthesized (Fig. 1). Quantitative structure activity relationships of these an-

alogues were defined and corresponded to those observed for the parental compounds. These ligand molecules were subsequently used as photoprobes, which led to the identification of protein regions contributing to the binding-domain of propafenone analogs.

Materials and Methods

Design and Synthesis of Compounds. Synthesis of compounds GPV05 to GPV180 was achieved as described previously (Chiba et al. 1995, 1996; Tmej et al., 1998). Benzophenone derivatives were synthesized in analogy to the procedures for GPV317 and GPV319 as outlined in Scheme 1 (Tmej et al., 1998). Thus, a corresponding 2-hydroxy-benzophenone (1) is reacted with epichlorohydrin to give the epoxide 2. Subsequent nucleophilic ring opening with piperidine yields the desired aminoalcohols (B59, BP11). Thieno-derivative BP01 was synthesized in an analogous manner. In the case of the pyrazine analog B47, the corresponding 2-chloro derivative was used instead of the hydroxy-derivative. In this case, formation of the epoxide was achieved with 2,3-epoxypropanol. The desoxy-analog BP23 was obtained via reaction of BP59 with hydroxylamine hydrochloride followed by hydrogenation of the oxime 3.

The phenolic precursor for the 5-methyl-analogs GPV442 and GPV443 was synthesized via acylation of 4-methylphenol (4) followed by Fries rearrangement of the phenylester 5 (Scheme 2). The permanently charged ammonium derivative GPV708 was obtained via methylation of the corresponding diethylamino-derivative (Chiba 1995). IR, MS, NMR spectroscopy and elemental analysis confirmed the structure of all novel compounds. ¹H-NMR spectra are given in Table 1. Structures are represented in Table 2.

Calculation of logP Values. The logP values were calculated using the software package ChemOffice (option: best method; CambridgeSoft Corporation, Cambridge, MA). Calculated logP values are given in Table 2.

Cell Lines. The human T-lymphoblast cell line CCRF-CEM and the multidrug resistant lines CCRF vcr1000 and CCRF adr5000 were provided by V. Gekeler (Byk Gulden, Konstanz, Germany). The resistant lines were obtained by stepwise selection in vincristine- or daunorubicin-containing medium (Boer et al., 1996). Cells were kept under standard culture conditions (RPMI 1640 medium supplemented with 10% fetal calf serum). The Pgp-expressing resistant cell lines were cultured in the presence of 1000 ng/ml vincristine or 5000 ng/ml daunorubicin, respectively. One week before the experiments, cells were transferred into medium without selective agents or antibiotics. Insect Sf9 cells were obtained from the American Type Culture Collection (Manassas, VA).

Daunorubicin Efflux Studies. Daunorubicin efflux studies were performed as described previously (Chiba et al., 1996). Briefly, cells were pelleted, the supernatant was removed by aspiration, and cells were resuspended at a density of 1×10^6 /ml in RPMI 1640 medium containing 3 μ M daunomycin. Cell suspensions were incu-

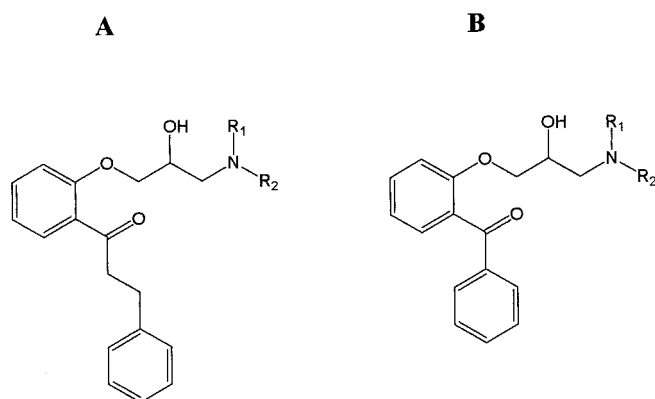
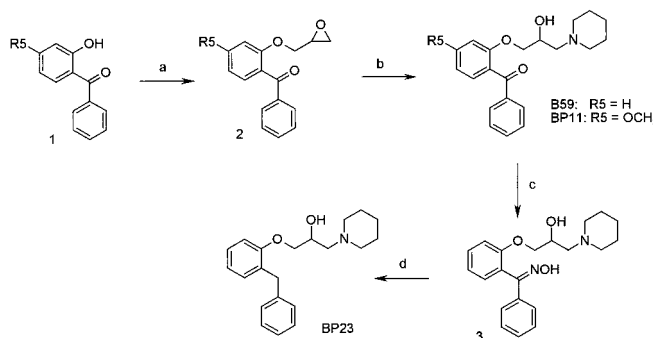
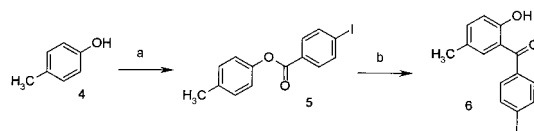


Fig. 1. General chemical structure of propafenone-type analogs and corresponding benzophenone photoaffinity ligands



Scheme 1. Synthesis of benzophenone derivatives. a, NaOH/epichlorohydrin; b, piperidine/MeOH; c, H₂NOH-HCl/EtOH; d, H₂/Pd-C/EtOH-MeOH (or Na/1-propanol).



Scheme 2. Synthesis of 5-methyl precursors. a, 4-Iodobenzoic acid chloride/pyridine; b, $\text{AlCl}_3/160^\circ\text{C}$.

bated at 37°C for 30 min. After this time, a steady state of daunorubicin accumulation was reached. Tubes were chilled on ice and cells were pelleted at 500g. Cells were washed once in RPMI 1640 medium to remove extracellular daunorubicin. Subsequently, cells were resuspended in medium prewarmed to 37°C , containing either no modulator or chemosensitizer at various concentrations ranging from 3 nM to 500 μM , depending on solubility and expected potency of the modifier. Generally, eight serial dilutions were tested for each modulator. After 1, 2, 3, and 4 min, aliquots of the incubation mixture were drawn and pipetted into 4 volumes of ice-cold stop solution (RPMI 1640 medium containing verapamil at a final concentration of 100 μM). Parental CCRF-CEM cells were used to correct for simple membrane diffusion, which was less than 3% of the efflux rate observed in resistant cells. Samples drawn at the respective time points were kept in an ice water bath and measured within an hour on a FACSCalibur (BD Biosciences, Heidelberg, Germany) flow cytometer as described. Dose-response curves were fitted to the data points using nonlinear least-squares and EC_{50} values were calculated as described previously (Chiba et al., 1996). EC_{50} values of individual compounds are given in Table 2 and represent the average and S.D. of at least triplicate determinations.

Irradiation Inactivation of Pgp. Whole cells were preincubated with ligand for 5 min at room temperature, placed on ice, and irradiated intermittently (six times for 30 s each) with a 500-W mercury lamp (Lot-Oriel, Darmstadt, Germany) in the presence and absence of the photoactivatable benzophenone analog GPV51. A 1-mm glass plate was placed in the light path to filter most of the UV light with wavelengths below 300 nm. The nonphotoactivatable analog GPV90 was included in duplicate samples at 100-fold molar excess for each individual concentration of GPV51 to prove the specificity of the reaction. Subsequently, unbound ligand was removed by

three consecutive washes in 100% fetal bovine serum at 37°C . Rhodamine 123 was added to give a final concentration of 0.52 μM and cells were incubated at 37°C for 30 min, after which time a steady state of fluorochrome uptake was reached. Cells were chilled in ice water and washed once with ice-cold RPMI1640 medium. Mean fluorescence units per cell were determined by use of the attractor software in a FACSCalibur flow cytometer (BD Biosciences).

Radiolabeling of Pgp with [^3H]GPV51 and Gel Electrophoretic Separation Conditions. Plasma membrane (PM) preparations of Sf9 cells transfected with the baculovirus construct containing the his-tagged *mdr1* gene (Germann et al., 1990) were prepared by nitrogen cavitation and subsequent discontinuous sucrose-gradient centrifugation as described previously (Schmid et al., 1999). PM vesicles were taken up in phosphate-buffered saline and preincubated with [^3H]GPV51 (5 μCi ; final concentration, 2.75 μM) for 30 min at ambient temperature. Subsequently, samples were irradiated under conditions identical to those described above. Unlabeled GPV51 or GPV90 was added at 100-fold molar excess. After irradiation, samples were centrifuged at 50,000g for 30 min at 4°C . Protein pellets were taken up in 1 \times SDS/sample buffer, loaded on 7.5% polyacrylamide gels, and run at 35 mA for 60 min using a Hoefer Mighty Small II SE250 unit (Amersham Biosciences, Vienna, Austria). Gels were fixed in methanol/glacial acetic acid/water (50:10:40) for 30 min, washed overnight in double-distilled water, and soaked in Amplify (Amersham Biosciences) for 30 min. Gels were dried for 2 h in a vacuum gel dryer (Bio-Rad, Vienna, Austria) at 80°C and subjected to fluorography using an Amersham enhanced chemiluminescence Hyperfilm.

Chemicals for In-Gel Digestion and Mass Spectrometry. High-quality water for the in-gel digestion and the mass spectrometric experiments was prepared using a Milli-Q water purification system (Millipore, Bedford, MA). Ammonium hydrogen carbonate was obtained from FLUKA (Sigma-Aldrich, Vienna, Austria), dithiothreitol for the reduction of proteins before in-gel digestion was purchased from Serva (Novex, San Diego, CA), iodoacetamide was supplied by Sigma-Aldrich, sequencing grade trypsin and chymotrypsin was obtained from Roche Diagnostics GmbH (Mannheim, Germany). Acetone was supplied by AppliChem (Darmstadt, Germany). High-performance liquid chromatography-grade acetonitrile,

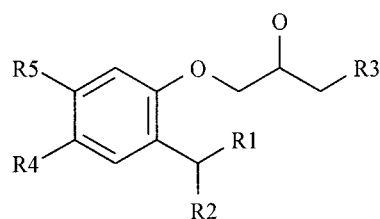
TABLE 1
NMR spectra of newly synthesized compounds

Compound	Formula	$^1\text{H-NMR}$; chloroform- d , δ (ppm)
BP001	$\text{C}_{19}\text{H}_{23}\text{NO}_3\text{S}$	1.41 (m, 2H, Pip H-4), 1.52 (m, 4H, Pip H-3, H-5), 2.06 (m, 2H, $-\text{CH}_2\text{-Pip}$), 2.19 and 2.39 (both m, 4H, Pip H-2, H-6), 2.94 (broad, 1H, OH), 3.74 (m, 1H, $-\text{CH-OH}$), 3.99 (d, 2H, $-\text{O-CH}_2\text{-}$), 6.87 (A, X-System, 1H, Th H-4), 7.42 (t, 2H, Ph H-3, H-5), 7.50 (t, 1H, Ph H-4), 7.56 (A, X-System, 1H, Th H-5), $^3J_{\text{H-4, H-5}} = 5.5$ Hz), 7.76 (d, 2H, Ph H-2, H-6)
B59	$\text{C}_{21}\text{H}_{25}\text{NO}_3$	1.39 (m, 2H, Pip H-4), 1.50 (m, 4H, Pip H-3, H-5), 2.02 (m, 2H, $-\text{CH}_2\text{-Pip}$), 2.34 and 2.17 (both m, 4H, Pip H-2, H-6), 3.43 (s, 1H, OH), 3.69 (m, 1H, $-\text{CH-OH}$), 3.87 (q, 1H, $-\text{O-CH}_2\text{-}$), 3.95 (q, 1H, $-\text{O-CH}_2\text{-}$), 6.98 (d, 1H, Ph H-3), 7.05 (t, 1H, Ph H-5), 7.42 (m, 2H, Ph' H-3, H-5), 7.43 (m, 1H, Ph H-6), 7.45 (m, 1H, Ph H-4), 7.53 (t, 1H, Ph' H-4), 7.77 (d, 2H, Ph' H-2, H-6)
B047	$\text{C}_{19}\text{H}_{23}\text{N}_3\text{O}_3$	1.43 (m, 2H, Pip H-4), 1.57 (m, 4H, Pip H-3, H-5), 2.36 (m, 2H, $-\text{CH}_2\text{-Pip}$), 2.54 and 2.35 (both m, 4H, Pip H-2, H-6), 4.02 (m, 1H, $-\text{CH-OH}$), 4.40 (m, 2H, $-\text{O-CH}_2\text{-}$), 7.46 (t, 2H, Ph H-3, H-5), 7.60 (t, 1H, Ph H-4), 7.86 (d, 2H, Ph H-2, H-6), 8.24 („s“, 2H, Pyraz H-5, H-6)
BP023	$\text{C}_{21}\text{H}_{27}\text{NO}_2$	1.47 (m, 2H, Pip H-4), 1.61 (m, 4H, Pip H-3, H-5), 2.38 (m, 2H, $-\text{CH}_2\text{-Pip}$), 2.57 and 2.36 (both m, 4H, Pip H-2, H-6), 3.56 (broad, 1H, OH), 3.92 (q, 1H, $-\text{O-CH}_2\text{-}$), 4.00 (m, 1H, $-\text{O-CH}_2\text{-}$), 4.00 (s, 2H, Ph- $\text{CH}_2\text{-Ph}$), 4.03 (m, 1H, $-\text{CH-OH}$), 6.87 (m, 1H, Ph H-3), 6.91 (m, 1H, Ph H-5), 7.12 (m, 1H, Ph H-6), 7.18 (m, 1H, Ph' H-4), 7.19 (m, 2H, Ph' H-2, H-6), 7.20 (m, 1H, Ph H-4), 7.26 (m, 2H, Ph' H-3, H-5)
BP011	$\text{C}_{22}\text{H}_{27}\text{NO}_4$	1.39 (m, 2H, Pip H-4), 1.50 (m, 4H, Pip H-3, H-5), 2.01 (m, 2H, $-\text{CH}_2\text{-Pip}$), 2.34 and 2.17 (both m, 4H, Pip H-2, H-6), 3.33 (broad, 1H, OH), 3.66 (m, 1H, $-\text{CH-OH}$), 3.85 (s, 3H, $-\text{OCH}_3$), 3.91 and 3.84 (q and m, 2H, $-\text{O-CH}_2\text{-}$), 6.50 (d, 1H, Ph H-3), 6.57 (dd, 1H, Ph H-5), $^4J_{\text{H-3, H-5}} = 2.2$ Hz), 7.40 (m, 2H, Ph' H-3, H-5), 7.46 (m, 1H, Ph H-6), $^3J_{\text{H-5, H-6}} = 8.5$ Hz), 7.51 (t, 1H, Ph' H-4), 7.73 (d, 2H, Ph' H-2, H-6)
GPV442	$\text{C}_{20}\text{H}_{25}\text{NO}_3$	0.87 (t, 3H, $^3J = 7.3$ Hz, $-\text{CH}_2\text{-CH}_3$), 1.46 (sx, 2H, $^3J = 7.3$ Hz, $-\text{CH}_2\text{-CH}_3$), 2.30 (s, 3H, $-\text{CH}_3$), 2.39-2.51 (m, 4H, $-\text{CH}_2\text{-N-CH}_2\text{-}$), 3.4 (br, 2H, OH, NH), 3.78-3.91 (m, 3H, $\text{O-CH}_2\text{-CH-}$), 6.87 (d, J = 8.4 Hz, Ph H-3), 7.20 (s, 1H, Ph H-6), 7.25 (d, 1H, J = 8.4 Hz, Ph H-4), 7.43 (t, 2H, J = 7.6 Hz, Ph' H-3, H-5), 7.55 (t, 1H, J = 7.5 Hz, Ph' H-4), 7.77 (t, 2H, J = 7.4 Hz, Ph' H-2, H-6)
GPV443	$\text{C}_{20}\text{H}_{24}\text{NO}_3\text{I}$	0.90 (t, 3H, $^3J = 7.3$ Hz, $-\text{CH}_2\text{-CH}_3$), 1.50 (sx, 2H, $^3J = 7.3$ Hz, $-\text{CH}_2\text{-CH}_3$), 2.29 (s, 3H, $-\text{CH}_3$), 2.37-2.54 (m, 4H, $-\text{CH}_2\text{-N-CH}_2\text{-}$), 3.83-3.93 (m, 5H, $\text{O-CH}_2\text{-CH-OH}$, OH, NH), 6.86 (d, 1H, J = 8.4 Hz, Ph H-3), 7.17 (s, 1H, Ph H-6), 7.25 (d, 1H, J = 8.4 Hz, Ph H-4), 7.47 (d, 2H, J = 8.4 Hz, Ph' H-3, H-5), 7.78 (d, 2H, J = 8.4 Hz, Ph' H-2, H-6)
GPV708	$\text{C}_{21}\text{H}_{28}\text{NO}_3\text{I}$	1.32 (t, 6H, J = 7.2 Hz, $2 \times -\text{CH}_2\text{-CH}_3$), 3.16 (s, 3H, $\text{N}^+\text{-CH}_3$), 3.37-3.64 (m, 6H, $-\text{CH}_2\text{-N}^+\text{-(CH}_2)_2$), 4.03-4.11 (m, 1H, J = O-CH_3), 4.31 (dd, 1H, J = 4.3/10.8 Hz, O-CH_2), 4.6-4.75 (m, 1H, CH(OH)), 7.05 (d, 1H, Ph H-3), 7.11 (t, 1H, Ph H-5), 7.38 (m, 1H, Ph H-6), 7.48-68 (m, 4H, Ph' H-3, H-4, H-5, Ph H-4), 7.85 (d, 2H, Ph' H-2, H-6)

TABLE 2

Chemical structure and calculated logP and EC₅₀ values for daunorubicin efflux inhibition of propafenone analogs and related compounds.

General structure



Compound	R ¹	R ²	R ³	R ⁴	R ⁵	calcd.logP (ChemDraw)	EC ₅₀ μmol/l
GPV05 ¹	=O			H	H	3.67	0.53 ± 0.03
GPV12 ¹	=O			H	H	2.07	6.55 ± 0.4
GPV17 ¹	=O			H	H	1.42	22.7 ± 0.85
GPV51 ²	=O			H	H	3.26	2.17 ± 0.15
GPV90 ¹	-OCH ₃			H	H	4.30	0.17 ± 0.04
GPV180 ³	=O			H	H	4.67	0.14 ± 0.06
GPV317 ³	=O			H	H	3.62	0.31 ± 0.005
GPV319 ³	=O			H	H	4.57	0.15 ± 0.039

methanol, and isopropanol were purchased from Sigma-Aldrich, trifluoroacetic acid was obtained from Pierce (Rockford, IL), and formic acid was supplied by Merck (Merck KGaA; Darmstadt, Germany). The α -cyano-4-hydroxycinnamic acid (CHCA) matrix for the MALDI-TOF MS measurements was acquired from Bruker Daltonik GmbH (Bremen, Germany) and was used without further purification. Nitrocellulose was purchased from Bio-Rad (Hercules, CA). Protein and peptide standards used to calibrate the MALDI mass spectrometer were acquired from Applied Biosystems (Foster City, CA).

Silver Staining and In-Gel Digestion. The silver staining was carried out according to the method of Shevchenko et al. (1996) and the in-gel digestion was executed without destaining of the gel as described in Durauer et al. (2000).

MALDI-TOF Mass Spectrometry. The mass spectrometer used in this work was a REFLEX III (Bruker Daltonik GmbH) MALDI-TOF instrument, equipped with a standard nitrogen laser (337 nm). The spectra were recorded in reflectron mode, positive ionization, and with 25-kV acceleration voltage. The laser power was varied on

TABLE 2
Continued.

GPV442	=O		-CH ₃	H	3.51	1.21 ± 0.253
GPV443	=O		-CH ₃	H	4.87	0.19 ± 0.005
GPV708	=O		H	H		58.0 ± 4.8
BP11	=O		H	-OCH ₃	3.19	0.55 ± 0.065
BP23	H		H	H	4.20	1.15 ± 0.169
B59	=O		H	H	3.31	1.20 ± 0.72
Compound	Structure				calcd.logP (ChemDraw)	EC ₅₀ μmol/l
BP01					3.29	1.17 ± 1.1
B47					1.78	9.09 ± 0.11

¹ Chiba et al. (1996).

² Chiba et al. (1995).

³ Tmej et al. (1998).

a relative scale of 0 to 100 and was kept at the threshold value to obtain appropriate signal intensity. The calibration of the instrument was done externally with [M+H]⁺ ions of des-Arg-bradykinin, angiotensin I, Glu-fibrinopeptide B, and adrenocorticotropin (clips 1–17 and 18–39). The samples were prepared with a 75:25 (v/v) mixture of CHCA matrix (saturated solution in acetone) and nitrocellulose [10 mg/ml solution in acetone-isopropanol 50:50 (v/v)] solutions. One microliter of the mixture was placed onto the sample slide and allowed to dry at room temperature. Part of the aliquot (0.5 μl) of the in-gel digestion was mixed with 0.5 μl 0.1% TFA on this thin layer of matrix crystals and was dried by the application of vacuum. Samples were washed with ice-cold 0.1% TFA. Hydrophobic peptides were purified and concentrated on Poros 20 R1 material (Applied Biosystems) loaded into GeLoader tips (Eppendorf-Netheler-Hinz-GmbH, Hamburg, Germany). The chromatography material was conditioned with 0.1% TFA and the peptides were eluted with CHCA

matrix [saturated solution in 0.1% TFA-acetonitrile 50:50 (v/v)] directly onto the sample slide. Each spectrum was produced by accumulating data from 90 to 120 consecutive laser shots. Monoisotopic mass values are reported in Table 3. Spectra were interpreted with the aid of the Mascot (Matrix Science Ltd, London, UK) or MS-Fit (Clauser et al., 1999) software using the NR database (NCBI Resources, National Institutes of Health, Bethesda, MD).

Results

QSAR of Photoligands. The arylcarbonyl substructure is common to PAs and benzophenones. This allowed the design of benzophenone analogs, which share the pharmacophoric carbonyl group with propafenone and are photoactivatable upon irradiation at a wavelength of 360 nm. Figure 2 shows

TABLE 3

Ligand-modified peptide fragments identified by MALDI-TOF mass spectrometry

<i>m/z</i> (mi) [M + H] ⁺		Mass Accuracy	Modif.	Start	End	E	Ligand	AA Sequence
Submitted	Matched							
<i>ppm</i>								
TM3				194	208			<u>FQSMATFFFTGFI</u> VGFTRGW
1174.610	1174.546	54	M-ox	194	200	C	GPV51	FQSMATFFFTGFI VGFTRGW
1173.599	1173.581	15		194	200	C	GPV708	FQSMATFFFTGFI VGFTRGW
1412.744	1412.640	74		194	201	C	GPV319	FQSMATFFFTGFI VGFTRGW
1641.865	1641.782	51	M-ox	194	204	C	GPV708	FQSMATFFFTGFI VGFTRGW
1127.550	1127.503	42		195	200	C	GPV319	FQSMATFFFTGFI VGFTRGW
1141.562	1141.525	32	pGlu	195	201	C	GPV51	FQSMATFFFTGFI VGFTRGW
1174.610	1174.546	54	M-ox	195	201	C	GPV51	FQSMATFFFTGFI VGFTRGW
1173.632	1173.581	43		195	201	C	GPV708	FQSMATFFFTGFI VGFTRGW
1505.787	1505.699	58		195	204	C	BP11	FQSMATFFFTGFI VGFTRGW
1462.691	1462.657	23	M-ox	195	204	C	GPV51	FQSMATFFFTGFI VGFTRGW
				pGlu				
1446.660	1446.662	−1	pGlu	195	204	C	GPV51	FQSMATFFFTGFI VGFTRGW
1446.720	1446.662	40	pGlu	195	204	C	GPV442	FQSMATFFFTGFI VGFTRGW
1462.726	1462.657	47	M-ox	195	204	C	GPV442	FQSMATFFFTGFI VGFTRGW
				pGlu				
1477.785	1477.687	66	M-ox	195	204	C	GPV708	FQSMATFFFTGFI VGFTRGW
			pGlu					
1920.940	1920.909	16	M-ox	195	208	C	BP11	FQSMATFFFTGFI VGFTRGW
				pGlu				
1969.900	1969.925	−13	pGlu	195	208	C	GPV319	FQSMATFFFTGFI VGFTRGW
1821.988	1821.916	40		201	212	C	GPV319	FQSMATFFFTGFI VGFTRGW
1240.691	1240.684	6		202	212	C	GPV51	FQSMATFFFTGFI VGFTRGW
1067.600	1067.578	21		202	208	C	GPV51	FQSMATFFFTGFI VGFTRGW
878.469	878.461	9		202	208	C	GPV319	FQSMATFFFTGFI VGFTRGW
866.520	866.471	57		205	208	C	GPV317	FQSMATFFFTGFI VGFTRGW
762.414	762.441	−35		205	208	C	GPV442	FQSMATFFFTGFI VGFTRGW
CL2				272	291			KELERYNKNLEEAKRIGIKK
2354.093	2354.230	−58		272	286	T	GPV319	KELERYNKNLEEAKRIGIKK
1320.590	1320.680	−68		273	279	T	BP11	KELERYNKNLEEAKRIGIKK
1278.689	1278.670	15		273	279	T	GPV51	KELERYNKNLEEAKRIGIKK
1978.010	1978.044	−17		273	285	T	GPV708	KELERYNKNLEEAKRIGIKK
1072.542	1072.553	−10		273	285	T	BP11	KELERYNKNLEEAKRIGIKK
1134.658	1134.573	75		280	285	T	GPV317	KELERYNKNLEEAKRIGIKK
989.570	989.608	−38		287	291	T	GPV317	KELERYNKNLEEAKRIGIKK
TM5				304	316			<u>LLIYASYALAFWY</u>
890.499	890.524	−28		304	307	C	BP11	LLIYASYALAFWY
1211.699	1211.656	35		304	310	C	BP11	LLIYASYALAFWY
1276.675	1276.666	7		304	310	C	GPV319	LLIYASYALAFWY
1571.770	1571.873	−66		304	314	C	GPV51	LLIYASYALAFWY
1282.670	1282.694	−19		305	312	C	BP11	LLIYASYALAFWY
1240.691	1240.684	6		305	312	C	GPV51	LLIYASYALAFWY
1500.807	1500.799	5		305	314	C	BP11	LLIYASYALAFWY
1127.596	1127.599	−3		306	312	C	GPV442	LLIYASYALAFWY
1127.640	1127.599	36		306	312	C	GPV51	LLIYASYALAFWY
1345.668	1345.705	−27		306	314	C	GPV442	LLIYASYALAFWY
1694.817	1694.872	−32		306	314	C	GPV51	LLIYASYALAFWY
1345.710	1345.705	4		306	316	C	GPV51	LLIYASYALAFWY
1173.660	1173.588	61		308	314	C	GPV317	LLIYASYALAFWY
1297.738	1297.647	70		308	315	C	BP11	LLIYASYALAFWY
1418.731	1418.700	22		308	316	C	GPV51	LLIYASYALAFWY
1201.679	1201.598	67		311	316	C	GPV317	LLIYASYALAFWY
TM6				327	343			<u>SIGQVLTVFFSVLIGAF</u>
1479.831	1479.810	14		327	336	C	BP11	SIGQVLTVFFSVLIGAF
1290.642	1290.732	−70		327	335	C	GPV51	SIGQVLTVFFSVLIGAF
1634.804	1634.867	−39		333	343	C	GPV319	SIGQVLTVFFSVLIGAF
1222.719	1222.672	38		336	343	C	BP11	SIGQVLTVFFSVLIGAF
1033.577	1033.594	−16		337	343	C	GPV51	SIGQVLTVFFSVLIGAF
749.433	749.413	27		337	339	C	GPV317	SIGQVLTVFFSVLIGAF
TM8				755	784			<u>FSLLFLALGIIISFITFFLQGF</u> TFGKAGEIL
995.486	995.545	−59		755	759	C	BP11	FSLLFLALGIIISFITFFLQGF TFGKAGEIL
1066.537	1066.619	−77		755	760	C	GPV51	FSLLFLALGIIISFITFFLQGF TFGKAGEIL
1292.747	1292.751	−3		755	762	C	BP11	FSLLFLALGIIISFITFFLQGF TFGKAGEIL
919.510	919.551	−45		756	760	C	GPV442	FSLLFLALGIIISFITFFLQGF TFGKAGEIL
1103.669	1103.672	−3		756	762	C	GPV442	FSLLFLALGIIISFITFFLQGF TFGKAGEIL
1066.537	1066.619	−77		756	762	C	GPV51	FSLLFLALGIIISFITFFLQGF TFGKAGEIL
1462.777	1462.856	−54		758	767	C	BP11	FSLLFLALGIIISFITFFLQGF TFGKAGEIL
1202.728	1202.704	20		760	767	C	BP11	FSLLFLALGIIISFITFFLQGF TFGKAGEIL
1160.646	1160.694	−41		760	767	C	GPV442	FSLLFLALGIIISFITFFLQGF TFGKAGEIL
967.446	967.518	−74		763	767	C	GPV317	FSLLFLALGIIISFITFFLQGF TFGKAGEIL
1266.741	1266.699	33		763	770	C	BP11	FSLLFLALGIIISFITFFLQGF TFGKAGEIL
1239.636	1239.719	−67		763	770	C	GPV708	FSLLFLALGIIISFITFFLQGF TFGKAGEIL
1413.774	1413.767	5		763	771	C	BP11	FSLLFLALGIIISFITFFLQGF TFGKAGEIL
1475.732	1475.787	−37		763	771	C	GPV317	FSLLFLALGIIISFITFFLQGF TFGKAGEIL
1920.922	1921.020	−51		763	775	C	GPV317	FSLLFLALGIIISFITFFLQGF TFGKAGEIL
896.448	896.477	−32		768	771	C	BP11	FSLLFLALGIIISFITFFLQGF TFGKAGEIL

TABLE 3

Continued

<i>m/z</i> (mi) [M + H] ⁺		Mass Accuracy	Modif.	Start	End	E	Ligand	AA Sequence
Submitted	Matched							
<i>ppm</i>								
967.481	967.551	-72		768	772	C	GPV51	FSLFLALGIIISF ITFFLQ GFTFGKAGEIL
980.487	980.509	-22		771	775	C	BP11	FSLFLALGIIISF ITFFLQ GFTFGKAGEIL
1290.663	1290.645	14		771	777	C	GPV317	FSLFLALGIIISF ITFFLQ GFTFGKAGEIL
1854.949	1855.001	-28		771	784	C	GPV51	FSLFLALGIIISF ITFFLQ GFTFGKAGEIL
791.446	791.431	19		772	775	C	GPV442	FSLFLALGIIISF ITFFLQ GFTFGKAGEIL
909.504	909.436	75		773	777	C	GPV442	FSLFLALGIIISF ITFFLQ GFTFGKAGEIL
1118.567	1118.503	57		778	784	C	GP319	FSLFLALGIIISF ITFFLQ GFTFGKAGEIL
CL3								
				789	798			RYMVFRSMLR
1084.622	1084.550	66		789	793	T	BP11	RYMVFRSMLR
1042.570	1042.540	29		789	793	T	GPV442	RYMVFRSMLR
1042.524	1042.540	-15		789	793	T	GPV51	RYMVFRSMLR
1545.756	1545.793	-24	M-ox	789	797	T	GPV51	RYMVFRSMLR
1649.821	1649.823	-1	M-ox	790	798	T	GPV317	RYMVFRSMLR
1561.780	1561.788	-5	2 M-ox	790	798	T	GPV51	RYMVFRSMLR
1225.643	1225.663	-16		791	797	C	GPV708	RYMVFRSMLR
TM10								
				852	862			IYGWQLTLLLL
1650.797	1650.919	-74		852	861	C	GPV317	IYGWQLTLLLL
784.453	784.446	9		856	859	C	GPV442	IYGWQLTLLLL
801.442	801.473	-39		856	859	C	GPV51	IYGWQLTLLLL
956.609	956.567	44		856	860	C	BP11	IYGWQLTLLLL
1025.578	1025.644	-64		856	861	C	GPV708	IYGWQLTLLLL
1182.710	1182.735	-21		856	862	C	BP11	IYGWQLTLLLL
1230.694	1230.776	-67		856	862	C	GPV319	IYGWQLTLLLL
786.487	786.498	-14		858	861	C	GPV442	IYGWQLTLLLL
1003.590	1003.612	-22		858	862	C	GPV317	IYGWQLTLLLL
TM11/12								
				939	984			GITFSFTQAMMYFSYAGCFRFGAYLVAHKLMSEFEDVLLVFSAVVFGAMAVGQVSSF
ECL6								
								TM11 ECL6 TM12
764.428	764.420	10		939	942	C	GPV51	GITFSFTQAMMYFSYAGCFRFGAYLVAHKLMSEFEDVLLVFSAVVFGAMAVGQVSSF
1859.902	1859.828	40	2 M-ox	939	950	C	GPV317	GITFSFTQAMMYFSYAGCFRFGAYLVAHKLMSEFEDVLLVFSAVVFGAMAVGQVSSF
2010.016	2009.886	65	2 M-ox	939	951	C	GPV319	GITFSFTQAMMYFSYAGCFRFGAYLVAHKLMSEFEDVLLVFSAVVFGAMAVGQVSSF
1870.990	1870.877	60		939	951	C	GPV442	GITFSFTQAMMYFSYAGCFRFGAYLVAHKLMSEFEDVLLVFSAVVFGAMAVGQVSSF
1887.027	1886.871	83	M-ox	939	951	C	GPV442	GITFSFTQAMMYFSYAGCFRFGAYLVAHKLMSEFEDVLLVFSAVVFGAMAVGQVSSF
1870.881	1870.877	2		939	951	C	GPV51	GITFSFTQAMMYFSYAGCFRFGAYLVAHKLMSEFEDVLLVFSAVVFGAMAVGQVSSF
1886.867	1886.871	-2	M-ox	939	951	C	GPV51	GITFSFTQAMMYFSYAGCFRFGAYLVAHKLMSEFEDVLLVFSAVVFGAMAVGQVSSF
2162.869	2162.982	-52		939	953	C	BP11	GITFSFTQAMMYFSYAGCFRFGAYLVAHKLMSEFEDVLLVFSAVVFGAMAVGQVSSF
978.472	978.407	66		943	950	C	GPV51	GITFSFTQAMMYFSYAGCFRFGAYLVAHKLMSEFEDVLLVFSAVVFGAMAVGQVSSF
1452.753	1452.655	67		943	951	C	GPV51	GITFSFTQAMMYFSYAGCFRFGAYLVAHKLMSEFEDVLLVFSAVVFGAMAVGQVSSF
1760.847	1760.755	52	M-ox	943	953	C	BP11	GITFSFTQAMMYFSYAGCFRFGAYLVAHKLMSEFEDVLLVFSAVVFGAMAVGQVSSF
1118.572	1118.506	59	2 M-ox	945	950	C	GPV708	GITFSFTQAMMYFSYAGCFRFGAYLVAHKLMSEFEDVLLVFSAVVFGAMAVGQVSSF
1338.646	1338.579	50	M-ox	945	951	C	GPV317	GITFSFTQAMMYFSYAGCFRFGAYLVAHKLMSEFEDVLLVFSAVVFGAMAVGQVSSF
1935.685	1935.797	-58	2 M-ox	945	957	C	GPV51	GITFSFTQAMMYFSYAGCFRFGAYLVAHKLMSEFEDVLLVFSAVVFGAMAVGQVSSF
847.446	847.392	64		951	953	C	GPV317	GITFSFTQAMMYFSYAGCFRFGAYLVAHKLMSEFEDVLLVFSAVVFGAMAVGQVSSF
1496.788	1496.719	46		951	959	C	GPV708	GITFSFTQAMMYFSYAGCFRFGAYLVAHKLMSEFEDVLLVFSAVVFGAMAVGQVSSF
1772.856	1772.811	25		951	962	C	GPV442	GITFSFTQAMMYFSYAGCFRFGAYLVAHKLMSEFEDVLLVFSAVVFGAMAVGQVSSF
1767.856	1767.919	-36		960	971	C	GPV317	GITFSFTQAMMYFSYAGCFRFGAYLVAHKLMSEFEDVLLVFSAVVFGAMAVGQVSSF
1783.850	1783.914	-36	M-ox	960	971	C	GPV317	GITFSFTQAMMYFSYAGCFRFGAYLVAHKLMSEFEDVLLVFSAVVFGAMAVGQVSSF
1049.567	1049.636	-66		963	968	C	BP11	GITFSFTQAMMYFSYAGCFRFGAYLVAHKLMSEFEDVLLVFSAVVFGAMAVGQVSSF
1372.713	1372.767	-39		963	971	C	GPV442	GITFSFTQAMMYFSYAGCFRFGAYLVAHKLMSEFEDVLLVFSAVVFGAMAVGQVSSF
1870.896	1870.999	-55		963	975	C	BP11	GITFSFTQAMMYFSYAGCFRFGAYLVAHKLMSEFEDVLLVFSAVVFGAMAVGQVSSF
1886.904	1886.994	-48	M-ox	963	975	C	BP11	GITFSFTQAMMYFSYAGCFRFGAYLVAHKLMSEFEDVLLVFSAVVFGAMAVGQVSSF
1379.606	1379.708	-74	M-ox	964	971	C	GPV317	GITFSFTQAMMYFSYAGCFRFGAYLVAHKLMSEFEDVLLVFSAVVFGAMAVGQVSSF
1870.922	1870.999	-41		964	976	C	BP11	GITFSFTQAMMYFSYAGCFRFGAYLVAHKLMSEFEDVLLVFSAVVFGAMAVGQVSSF
1886.879	1886.994	-61	M-ox	964	976	C	BP11	GITFSFTQAMMYFSYAGCFRFGAYLVAHKLMSEFEDVLLVFSAVVFGAMAVGQVSSF
1366.692	1366.703	-8		964	971	C	GPV319	GITFSFTQAMMYFSYAGCFRFGAYLVAHKLMSEFEDVLLVFSAVVFGAMAVGQVSSF
1382.718	1382.698	14	M-ox	964	971	C	GPV319	GITFSFTQAMMYFSYAGCFRFGAYLVAHKLMSEFEDVLLVFSAVVFGAMAVGQVSSF
1167.625	1167.561	55		969	975	C	GPV442	GITFSFTQAMMYFSYAGCFRFGAYLVAHKLMSEFEDVLLVFSAVVFGAMAVGQVSSF
1167.639	1167.561	67		969	975	C	GPV51	GITFSFTQAMMYFSYAGCFRFGAYLVAHKLMSEFEDVLLVFSAVVFGAMAVGQVSSF
1384.770	1384.675	69		969	976	C	GPV317	GITFSFTQAMMYFSYAGCFRFGAYLVAHKLMSEFEDVLLVFSAVVFGAMAVGQVSSF
1280.683	1280.645	30		969	976	C	GPV442	GITFSFTQAMMYFSYAGCFRFGAYLVAHKLMSEFEDVLLVFSAVVFGAMAVGQVSSF
1296.723	1296.640	64	M-ox	969	976	C	GPV442	GITFSFTQAMMYFSYAGCFRFGAYLVAHKLMSEFEDVLLVFSAVVFGAMAVGQVSSF
1996.184	1996.133	26		969	976	C	GPV708	GITFSFTQAMMYFSYAGCFRFGAYLVAHKLMSEFEDVLLVFSAVVFGAMAVGQVSSF
705.409	705.419	-14		976	978	C	GPV51	GITFSFTQAMMYFSYAGCFRFGAYLVAHKLMSEFEDVLLVFSAVVFGAMAVGQVSSF
1312.625	1312.724	-75		976	983	C	GPV317	GITFSFTQAMMYFSYAGCFRFGAYLVAHKLMSEFEDVLLVFSAVVFGAMAVGQVSSF
705.409	705.419	-14		976	978	C	GPV319	GITFSFTQAMMYFSYAGCFRFGAYLVAHKLMSEFEDVLLVFSAVVFGAMAVGQVSSF
1208.654	1208.694	-33		976	983	C	GPV51	GITFSFTQAMMYFSYAGCFRFGAYLVAHKLMSEFEDVLLVFSAVVFGAMAVGQVSSF
1925.866	1925.968	-53		979	994	C	BP11	GITFSFTQAMMYFSYAGCFRFGAYLVAHKLMSEFEDVLLVFSAVVFGAMAVGQVSSF
2006.906	2006.937	-15		979	994	C	GPV319	GITFSFTQAMMYFSYAGCFRFGAYLVAHKLMSEFEDVLLVFSAVVFGAMAVGQVSSF
1500.745	1500.709	24		984	994	C	GPV317	GITFSFTQAMMYFSYAGCFRFGAYLVAHKLMSEFEDVLLVFSAVVFGAMAVGQVSSF
IDSYSTEGMLPNTLEGNVTF								

Table continued on next page.

the correlation of calculated logP values and the logarithm of the Pgp-inhibitory potency for a series of *ortho*-acylphenoxypipranolamines, with R being methyl, ethyl, phenyl, phenylethyl, or naphthylethyl (in order of increasing lipophilicity).

All data points are located within the 95% confidence interval of the linear regression line (dotted lines in Fig. 2). The high value of the correlation coefficient ($r^2 = 0.997$) demonstrates that R influences pharmacological activity

TABLE 3
Continued

<i>m/z</i> (mi) [M + H] ⁺		Mass Accuracy	Modif.	Start	End	E	Ligand	AA Sequence
Submitted	Matched							
<i>ppm</i>								
866.396	866.415	−22		1018	1021	C	BP11	IDS SYST E GLMPNT L EGNVTF
824.344	824.405	−74		1018	1021	C	GPV51	IDS SYST E GLMPNT L EGNVTF
1353.715	1353.643	−53		1018	1026	C	BP11	IDS SYST E GLMPNT L EGNVTF
1311.554	1311.633	−60		1018	1026	C	GPV51	IDS SYST E GLMPNT L EGNVTF
1311.657	1311.633	18		1018	1026	C	GPV442	IDS SYST E GLMPNT L EGNVTF
1925.866	1925.905	−20		1018	1031	C	BP11	IDS SYST E GLMPNT L EGNVTF
1447.740	1447.699	28		1022	1031	C	BP11	IDS SYST E GLMPNT L EGNVTF
1389.686	1389.694	−6		1022	1031	C	GPV 51	IDS SYST E GLMPNT L EGNVTF
1389.667	1389.694	−19		1022	1031	C	GPV442	IDS SYST E GLMPNT L EGNVTF
1025.536	1025.481	54		1027	1031	C	GPV319	IDS SYST E GL M PNT L EGNVTF
1656.730	1656.778	−29		1027	1037	C	GPV319	IDS SYST E GL M PNT L EGNVTF
1564.807	1564.788	12		1027	1037	C	GPV708	IDS SYST E GL M PNT L EGNVTF

solely by its contribution to overall lipophilicity of the molecules. Thus, replacement of the phenylethyl group, which is characteristic for PAs, by phenyl, which renders the compound a benzophenone, is not critical with regard to the interaction of the carbonyl group.

In a next step, the phenylpropiophenone core structure was therefore replaced by benzophenone. Subsequently, the central aromatic ring system, the carbonyl group or substituents of the nitrogen atom were varied to prove that the structure-activity relationship pattern is retained for this subclass of compounds. Figure 3 shows a plot of calculated logP values versus log potency values for daunorubicin efflux inhibition. The solid line represents the linear relationship for a series of PAs, as established previously (Chiba et al., 1996). Six benzophenones with a broad variation in lipophilicity (logP 1.78–4.87) were located within or close to the 95% confidence interval represented by the dotted lines in Fig. 3.

Three of these six compounds were varied on the nitrogen atom (diethylamine (GPV51), piperidine (B59), and *p*-fluorophenylpiperazine (GPV319)). In two compounds (BP01, B47), the central aromatic ring was replaced by the bioisosteric structures thiophene or pyrazine, respectively. Compound GPV443, which carries an iodo atom attached to the benzophenone core, was designed as a potential radioligand. This modification did not lead to a change in the log potency/logP ratio.

GPV317 showed higher activity than predicted on basis of its logP value, which was due to the previously demonstrated beneficial effect of the hydroxyphenylpiperidine group (Tmej et al., 1998). Based on the favorable minus sigma effect of the methoxy group, which increases the hydrogen bond acceptor strength of the carbonyl oxygen, BP11 was also located above the correlation line. This is in agreement with results ob-

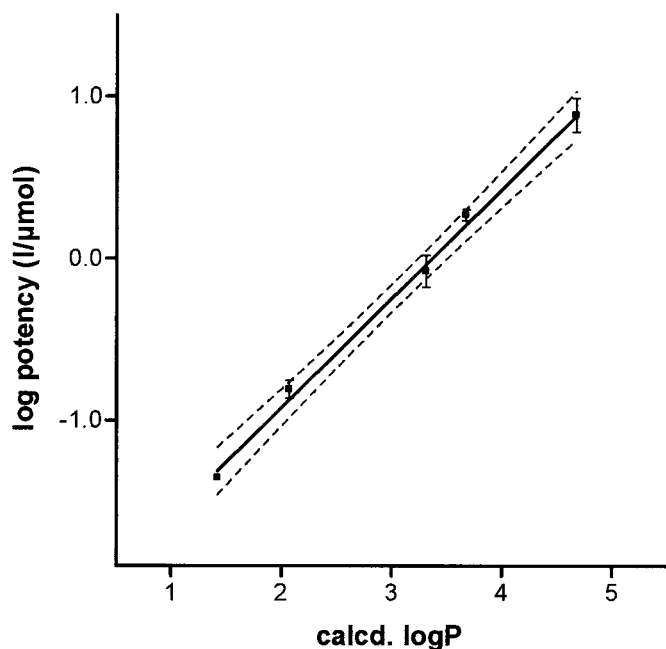


Fig. 2. Plot of calculated logP versus log potency for a series of *o*-acylphenoxypropanolamines with different substituent R2 (compare Table 2). Data points represent, in order of increasing lipophilicity, compounds GPV17 (methyl), GPV12 (ethyl), B59 (phenyl), GPV05 (phenylethyl), and GPV180 (naphthylethyl). The linear regression is shown as a solid line. Dotted lines represent the 95% confidence interval. Error bars are given for at least triplicate determinations. If not shown, error bars are located within symbols.

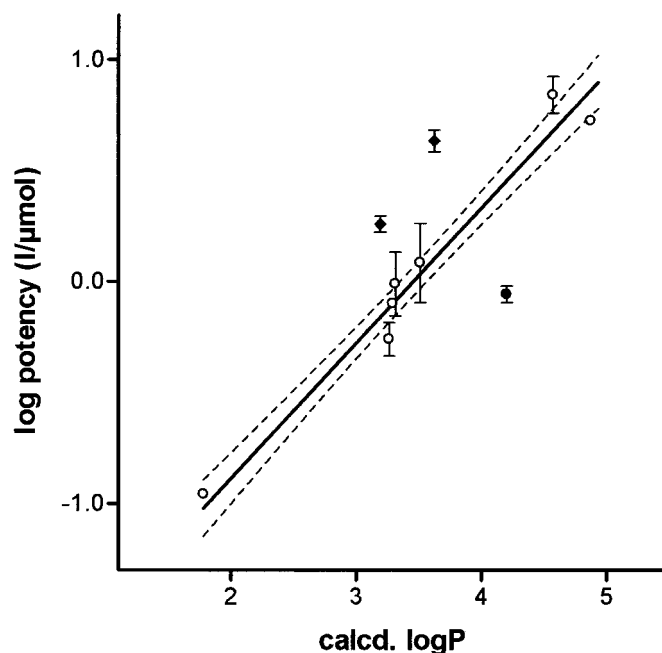


Fig. 3. Plot of calculated logP versus log potency for a series of benzophenone derivatives (○). The solid line represents the correlation line previously established for a series of PAs (cf. Chiba et al., 1996). Linear regression line and 95% confidence interval for substances 1c, 1d, 1e, 1g, 1h, 1i, 1k, and 1l). BP11 and GPV317 (◆) are compounds containing a benzophenone structure of which the corresponding phenylpropiophenone analogs have previously been shown to be located above the correlation line. BP23 (●) is the compound lacking a carbonyl oxygen. If not shown, error bars are located within symbols.

tained for the corresponding PAs (P. Chiba, G. Ecker, unpublished observations). Reductive removal of the carbonyl oxygen led to compound BP23, which showed an approximately 3.3-fold lower activity than predicted on basis of its lipophilicity. These data unequivocally demonstrate the importance of the carbonyl group as a pharmacophoric substructure.

Irreversible Inhibition of Pgp by Irradiation in the Presence of GPV51. Fig. 4 shows that irradiation of Pgp in the presence of GPV51 led to irreversible inactivation of Pgp function. A concentration-dependent increase in steady state fluorochrome accumulation was observed with increasing concentration of GPV51 (Fig. 4, ●). At each concentration of GPV51, a 100-fold molar excess of the nonphotoactivatable propafenone analog GPV90 prevented the inactivation of Pgp. This indicated high specificity of the photolabeling reaction (Fig. 4, △). A similar dose-dependent inactivation was observed with all other benzophenone analogs (data not shown). Under identical irradiation conditions, Pgp was not inactivated by phenylpropylphenones.

Radiolabeling of Plasma Membrane Proteins by [³H]GPV51 and Competition by Unlabeled GPV51 and GPV90. Pgp was separated in 7.5% polyacrylamide gels as described under *Materials and Methods*. The band corresponding to Pgp was visualized by silver staining, excised, and purity was assessed by MALDI-TOF MS fingerprinting. For samples in which plasma membrane vesicles were irradiated in the presence of [³H]GPV51, one major band was visible in fluorographs. By Western blotting, this band was confirmed to correspond to Pgp (data not shown). In Pgp-expressing CCRF T-lymphoblasts, the band had a molecular mass of 170 kDa (Fig. 5A, lane 1), whereas in Sf9 insect cells, in which the protein is only core glycosylated, Pgp migrated at 140 kDa (Fig. 5, B and C, lane 1). According to the specific activity of [³H]GPV51 (20 Ci/mmol), given the number of disintegrations per minute associated with the Pgp-band and an estimated protein amount of 10 ng, the labeling efficiency computed to be approximately 15% at a ligand concentration

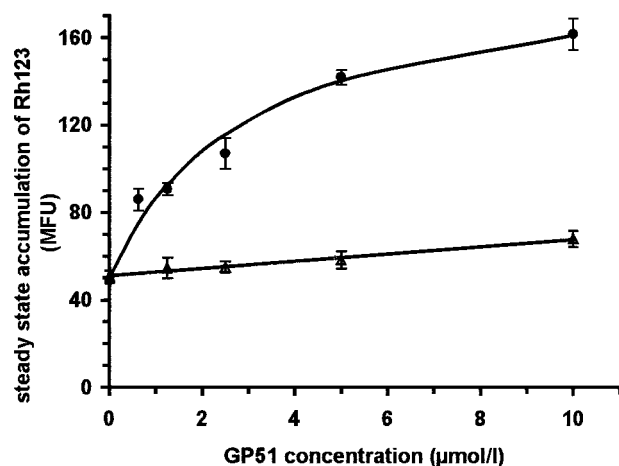


Fig. 4. Irreversible inactivation of Pgp by UV-irradiation in presence of the benzophenone GPV51. The steady-state accumulation levels of Rh123 are given as mean fluorescence units per cell at increasing concentration of GPV51 (●) and in the simultaneous presence of GPV51 and the non-photoactivatable analog GPV90 (△). Symbols and error bars represent the mean and S.D. of two independent experiments performed in duplicate. Samples in which Pgp was blocked by the addition of 10 μ M GPV31 served as controls (649 ± 108 mean fluorescence units) for complete inactivation.

of 2.75 μ M. This is in agreement with data obtained from irradiation inactivation experiments (cf. Fig. 4).

Nonradioactive GPV51 competed with [³H]GPV51 binding in a dose-dependent manner in both CCRF adr5000 T-lymphoblasts and baculovirus-transduced Sf9 insect cells (Fig. 5, A and B, lanes 2–8). Competition was visible starting at 12.8 μ M and was almost complete at 32 μ M. A similar picture was obtained when the nonphotoactivatable methoxy-derivative GPV90 was used as the competitor (Fig. 5C).

Identification of Ligand Modified Fragments by MALDI-TOF Mass Spectrometry. Six ligands (BP11, GPV51, GPV317, GPV319, GPV442, and GPV708) were used in subsequent photoaffinity labeling studies. After irradiation of PM vesicles in the presence of ligand, samples were separated by polyacrylamide gel electrophoresis and protein bands were visualized by silver staining. The band corresponding to Pgp was excised and digested with trypsin and chymotrypsin in separate reactions. Trypsin digests yielded protein fragments that were derived from putative cytoplas-

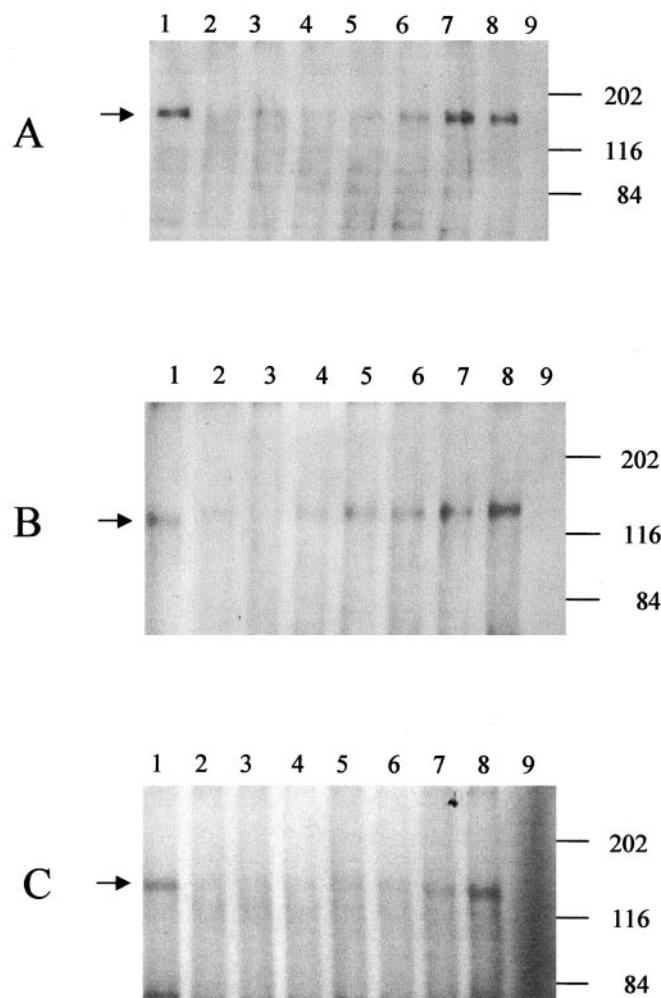


Fig. 5. Fluorography of 7.5% polyacrylamide gels of plasma membrane preparations of CCRF adr5000 cells (A) or Sf9-cells infected with the baculovirus vector containing the *mdr1* gene (B and C). The prominent band visible in samples irradiated in the presence of [³H]GPV51 is that corresponding to Pgp (arrows). In the presence of either unlabeled GPV51 (A and B) or GPV90 (C), intensity of the Pgp-band decreased. Concentrations of competitor were 500 μ M (lane 2), 200 μ M (lane 3), 80 μ M (lane 4), 32 μ M (lane 5), 12.8 μ M (lane 6), 5.1 μ M (lane 7), and 2.1 μ M (lane 8), respectively. Lane 9 represents unirradiated control samples.

mic (CL) and extracytoplasmic loops (ECL). An almost complete recovery of transmembrane segments was however obtained in chymotrypsin digested samples. The sequence coverage was approximately 50% for trypsin digests alone and nearly 60% for samples digested with chymotrypsin. When combining the sequence coverage obtained with either enzyme alone, more than 80% of the Pgp protein sequence was recovered. Identity of the protein fragments was supported by detection of complete and partial modifications of amino acid residues introduced during sample processing (compare Table 3). These were complete chemical modification of cysteine-residues (carbamidomethylation), partial oxidation of methionine residues and partial formation of pyroglutamic acid in peptides containing N-terminal glutamines. In addition, use of a set of ligands resulted in shifts of peptide mass peaks to different composite masses, depending on the exact mass of the respective ligand.

Unmatched fragment masses recovered in control samples (irradiated in the absence of photoaffinity ligands) were excluded from further consideration. Monoisotopic peak masses that did not correspond to unmodified Pgp fragments were then matched to the sum of the exact mass of the individual ligand and the monoisotopic mass of protein fragments obtained in *in silico* digests. Up to five missing enzyme cleavage sites were considered. Each sample was measured repeatedly. Additional measurements were performed on samples in which hydrophobic fragments were enriched by use of a reversed phase material as described under *Materials and Methods*. A representative mass spectrum is shown in Fig. 6.

Consensus labeling regions were defined by frequency distribution analysis, whereby the required number of ligands binding within these regions was set to a minimum of four of six. Results are summarized in Table 3. Submitted and matched peptide masses, mass accuracy in parts per million, position of start and end amino acid of the peptide fragment, amino acid sequence, and ligand and putative location within Pgp are specified. In addition, the enzyme used in digests is indicated (C, chymotrypsin; T, trypsin). The following protein regions were identified to contain covalently bound ligands: putative TM3 (AA residues 194–208), TM5 (AA 304–316), TM6 (AA 327–343), a region in putative TM8 extending seven amino acids into the C-terminal cytoplasmic loop 3 (CL3) (AA 755–784), TM10 (AA852–862), and a sequence stretching from AA 939 in TM11 to AA 994 in TM12 (including the extracytoplasmic loop 6). In addition, CL2 was labeled in a region confined to AA 272 to 291. All fragments recovered in the latter region showed an overlap with the so-called EAA-like motif, which is located between amino acids 278 and 294 (Shani et al., 1996). CL3 was labeled in the region extending from AA 789 to 798. In addition, overlapping fragments were found for the region spanning AA 1018 to 1037. With the exception of TM6 and TM12, in which ligand-modified fragments were identified for only four of six ligands, fragments covalently modified by either five or all six of the ligand molecules were found for the other regions. Multiple overlapping fragments were found within the specified regions (Table 3). In putative TM3 and TM11, as well as in CL3 and ECL6, fragments containing oxidized methionine residues were detected. Conversion of N-terminal glutamines to pyroglutamic acid was detectable for TM3 and occurred either alone or in combination with methionine oxidation. Because both modifications are partial, unmodified peptides

covering the same region were also recovered. Three cysteine-containing fragments that were accessible to ligand modification were recovered for putative TM11. These cysteines are chemically modified by carbamidomethylation during sample preparation. Correct mass-prediction for chemical modifications on one hand and varying (ligand-mass dependent) peak shifts on the other hand confirmed peptide identity.

Discussion

We studied the interaction of Pgp with low-molecular-mass ligands by designing a new class of photoactivatable molecules. PAs and benzophenones have in common an arylcarbonyl moiety. The carbonyl group was identified as a pharmacophore and evidence for an interaction via hydrogen bond formation was obtained (Chiba et al., 1996). This allowed the direct use of a pharmacophoric substructure as a photoactivatable group. Design of newly synthesized compounds was guided by replacement of the phenylpropiophenone core structure by benzophenone. The advantages of benzophenone

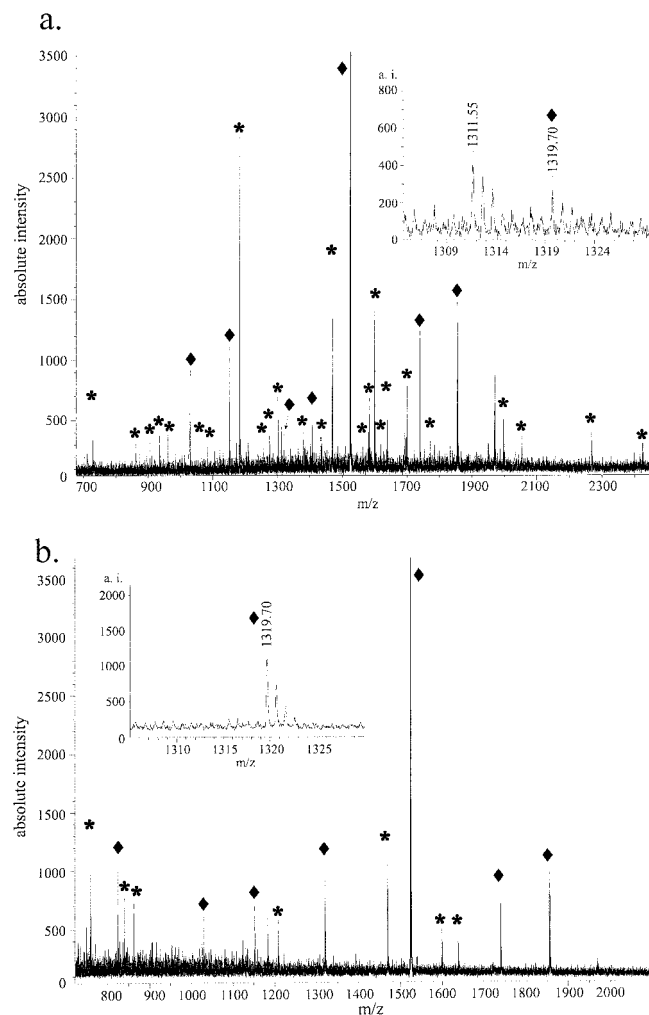


Fig. 6. Positive ion MALDI mass spectrum of chymotryptic peptides detected after the in-gel digestion of the modified (a) and control (b) Pgp. Identified, unmodified Pgp-peptides (*), as well as chymotrypsin autolysis peptides (◆) are labeled accordingly. Inset, presence of a modified peptide (IDSYSTEGL; AA 1018–1026) in the sample treated with the ligand GPV51 (a) that is absent in controls (b).

photochemistry were subject to comprehensive reviews by Dorman and Prestwich (1994, 2000).

To demonstrate a comparable structure-activity relationship pattern for both PAs and benzophenones, variations were introduced in the molecules on basis of previously defined pharmacophoric key features of PAs. These included modifications of the central aromatic ring system and the carbonyl group as well as variations in the vicinity of the nitrogen atom. As shown under *Results*, an analogous QSAR pattern was obtained for benzophenones and phenylpropionophenones (Figs. 2 and 3).

Irradiation of Pgp-expressing CCRF vcr1000 cells in the presence of these benzophenone ligands led to irreversible, dose-dependent inactivation of Pgp. This inactivation was reversed by the presence of the nonphotoactivatable methoxy analog GPV90. Results from both QSAR studies and irradiation inactivation experiments indicate identical binding domains for photoligands and propafenones.

When irradiated in the presence of tritiated GPV51, Pgp represented the major radiolabeled plasma membrane protein in fluorographs. Radiolabeling was competed by unlabeled GPV51 as well as the methoxy-derivative GPV90. This was initial evidence for the specificity of the labeling reaction.

Irradiation of Pgp in the presence of a set of photoligands, proteolytic in-gel digestion, and subsequent MALDI-TOF mass spectrometry led to the identification of a number of covalently modified protein fragments. Regions of the molecule, which are accessible to covalent ligand modification, include putative TM3, -5, -6, -8, -10, -11, and -12. In addition, confined regions in the second and third cytoplasmic loop as well as ECL6 and a region spanning AA 1018 to 1037 were found to bind the photoligands.

Earlier affinity labeling studies used analogs of vinblastine, the dihydropyridine azidopine, iodoarylazidoprazosine, forskolin and an iodinated derivative (iodoarylazidoprazosine-forskolin), tamoxifen aziridine, as well as two benzophenone analogs of paclitaxel. Comprehensive reviews on the subject have been published (Beck and Qian 1992; Dey et al., 1998; Greenberger, 1998; Safa, 1998). In combination with immunological mapping, these studies led to the identification of photoaffinity drug-binding epitopes. The position of the drug-binding domain in the N-terminal half of Pgp was proposed to span putative TM5 and TM6 (Greenberger, 1998). In the C-terminal half, ligand-binding regions have been reported to extend from the C terminus of TM11 to the N terminus of the Walker A motif of NBD2 (Greenberger, 1998). Isenberg et al. (2001) recently used [¹²⁵I]iodoarylazidoprazosine to obtain radioactively labeled peptide fragments that were isolated and sequenced. The authors identified amino acid regions 248 to 312 and 758 to 800 as being involved in binding of this radioligand.

Eight protein regions characterized in this study as contributing to the binding domain of propafenone analogs [AA272–286 (CL2), AA304–316 (TM5), AA327–343 (TM6), AA755–784 (TM8), AA789–798 (CL3), AA958–975 (ECL6), AA976–994 (TM12), and AA1018–1037] fall within those protein regions specified above as binding structurally different Pgp-photoligands.

The region extending from AA 272 to AA 286 in CL2 overlaps with a region known as the so-called EAA-like motif (Shani and Valle, 1996). Disease-producing mutations in hu-

man peroxisomal ABC transporters indicate the regions importance for functionality. On basis of sequence conservation and the results of mutational analysis, the EAA-like motif was suggested to mediate the interaction between TMD and NBD (Shani et al., 1996). Binding of substrate-type ligands within this region might thus be required for coupling ATP-binding and/or hydrolysis to substrate translocation.

Additional support for an involvement of putative TM5, -6, -10, -11, and -12 comes from data using cysteine-scanning mutagenesis in combination with substrate protection assays to characterize the drug binding domain of Pgp (Loo and Clarke, 2000, 2001b). A number of amino acid residues, which these authors proposed to be oriented toward the drug-binding domain shared by verapamil, vincristine, and colchicine, are located within regions of Pgp, which have now been identified as being accessible to covalent modification by propafenone analog-type photoaffinity ligands. These include I306 of putative TM5, L339 and A342 in TM6, as well as F942 and T945 in TM11 and L975, V982, G984, and A985 in TM12.

In conclusion, the present study demonstrates that the binding pattern for propafenone type analogs is distinct and is composed of regions that have previously been proposed to be involved in binding of other ligand molecules including vinblastine, cyclosporins, iodoarylazidoprazosine, verapamil, and colchicin.

The set of affinity ligands introduced in this study combines several favorable properties. First, molecules are intrinsically photoactivatable. Structural modification by insertion of a photoactivatable group is therefore unnecessary. Second, quantitative structure activity relationships have been well established for this group of compounds. Third, chymotrypsin digests yield a large number of protein fragments. However, use of a set of ligand molecules of different molecular mass allows accurate identification of consensus binding regions.

Finally, the quaternary compound GPV06 has previously been demonstrated to be a substrate for Pgp (Schmid et al., 1999). The analogous benzophenone GPV708 shows a labeling pattern that corresponds to that of the other ligand molecules. Therefore, this compound will provide a valuable tool for studying binding regions for substrate molecules at different stages of the catalytic cycle. Systematic ligand modification in combination with high-resolution mass spectrometry represents a powerful tool to obtain information on binding-domain organization and might thus link structural information at atomic resolution to functional aspects.

The ligand binding regions identified in this study contain hydrogen bond donors, such as T199, S309, S766, T862, T941, and Y950, that are highly conserved within mammalian P-glycoproteins. An interaction of Pgp with ligands via hydrogen bond formation has been demonstrated (Ecker et al., 1999; Seelig and Landwojtowicz, 2000). Upon addition of ATP, a relative repositioning of putative TM6 and -12 has recently been shown (Loo and Clarke, 2001a). Furthermore, repacking of the transmembrane domains of P-glycoprotein during the transport ATPase cycle has been demonstrated by electron cryomicroscopy (Rosenberg et al., 2001). We propose that this movement relocates the ligand from the hydrophobic membrane environment to the aqueous environment of the Pgp-chamber and that this relocation results in an instantaneous cleavage of hydrogen bonds by water molecules. The accompanying decrease in affinity might be the crucial

step leading to a release of the ligand-molecule from the protein. We believe that the availability of this set of ligand molecules will allow experimental testing of this hypothesis.

Acknowledgments

The baculovirus expression vector pVL941-MDR1/A was generously provided by Dr. M. M. Gottesman (National Cancer Institute, Bethesda, MD). We thank Andrea Barta for stimulating discussion. Dedicated to W. Fleishhacker and E. Kaiser.

References

- Balzi E, Wang M, Leterme S, Van Dyck L, and Goffeau A (1994) PDR5, a novel yeast multidrug resistance conferring transporter controlled by the transcription regulator PDR1. *J Biol Chem* **269**:2206–2214.
- Beck WT and Qian X-D (1992) Photoaffinity substrates for P-glycoprotein. *Biochem Pharmacol* **43**:89–93.
- Bissinger PH and Kuchler K (1994) Molecular cloning and expression of the *Saccharomyces cerevisiae* STS1 gene product. A yeast ABC transporter conferring mycotoxin resistance. *J Biol Chem* **269**:4180–4186.
- Boer R, Gekeler V, Ulrich WR, Zimmermann P, Ise W, Schodl A, and Haas S (1996) Modulation of P-glycoprotein mediated drug accumulation in multidrug resistant CCRF VCR-1000 cells by chemosensitisers. *Eur J Cancer* **32A**:857–861.
- Chiba P, Burghofer S, Richter E, Tell B, Moser A, and Ecker G (1995) Synthesis, pharmacologic activity, and structure-activity relationships of a series of propafenone-related modulators of multidrug resistance. *J Med Chem* **38**:2789–2793.
- Chiba P, Ecker G, Schmid D, Drach J, Tell B, Goldenberg S, and Gekeler V (1996) Structural requirements for activity of propafenone-type modulators in P-glycoprotein-mediated multidrug resistance. *Mol Pharmacol* **49**:1122–1130.
- Clauser KR, Baker PR, and Burlingame AL (1999) Role of accurate mass measurement (+/–10 ppm) in protein identification strategies employing MS or MS/MS and database searching. *Anal Chem* **71**:14, 2871–2882.
- Dey S, Hafkemeyer P, Pastan I, and Gottesman MM (1999) A single amino acid residue contributes to distinct mechanisms of inhibition of the human multidrug transporter by stereoisomers of the dopamine receptor antagonist flupentixol. *Biochemistry* **38**:6630–6639.
- Dey S, Ramachandra M, Pastan I, Gottesman MM, and Ambudkar SV (1998) Photoaffinity labeling of human P-glycoprotein: effect of modulator interaction and ATP hydrolysis on substrate binding. *Methods Enzymol* **292**:318–328.
- Dorman G and Prestwich GD (1994) Benzophenone photophores in biochemistry. *Biochemistry* **33**:5661–5673.
- Dorman G and Prestwich GD (2000) Using photolabile ligands in drug discovery and development. *Trends Biotechnol* **18**:64–77.
- Durauer A, Csaszar E, Mechtler K, Jungbauer A, and Schmid E (2000) Characterisation of the rubber elongation factor from ammoniated latex by electrophoresis and mass spectrometry. *J Chromatogr* **890**:145–148.
- Ecker G, Chiba P, Hitzler M, Schmid D, Visser K, Cordes HP, Csolleij J, Seydel JK, and Schaper KJ (1996) Structure-activity relationship studies on benzofuran analogs of propafenone-type modulators of tumor cell multidrug resistance. *J Med Chem* **39**:4767–4774.
- Ecker G, Huber M, Schmid D, and Chiba P (1999) The importance of a nitrogen atom in modulators of multidrug resistance. *Mol Pharmacol* **56**:791–796.
- Germann UA, Willingham MC, Pastan I, and Gottesman MM (1990) Expression of the human multidrug transporter in insect cells by a recombinant baculovirus. *Biochemistry* **29**:2295–2303.
- Gottesman MM and Pastan I (1993) Biochemistry of multidrug resistance mediated by the multidrug transporter. *Annu Rev Biochem* **62**:385–427.
- Greenberger LM (1998) Identification of drug interaction sites in P-glycoprotein. *Methods Enzymol* **292**:307–317.
- Isenberg B, Thole H, Tümmler B, and Demmer A (2001) Identification and localization of three photobinding sites of iodoarylazidoprazosin in hamster P-glycoprotein. *Eur J Biochem* **268**:2629–2634.
- Krishna R and Mayer LD (2000) Multidrug resistance (MDR) in cancer Mechanism, reversal using modulators of MDR and the role of MDR modulators in influencing the pharmacokinetics of anticancer drugs. *Eur J Pharmacol Sci* **11**:265–283.
- Lomovskaya O and Watkins W (2001) Inhibition of efflux pumps as a novel approach to combat drug resistance in bacteria. *J Mol Microbiol Biotechnol* **3**:225–236.
- Loo TW and Clarke DM (1998) Mutational analysis of human P-glycoprotein. *Methods Enzymol* **292**:480–492.
- Loo TW and Clarke DM (2000) Identification of residues within the drug-binding domain of the human multidrug resistance P-glycoprotein by cysteine-scanning mutagenesis and reaction with dibromobimane. *J Biol Chem* **275**:39272–39278.
- Loo TW and Clarke DM (2001a) Cross-linking of human multidrug resistance P-glycoprotein by the substrate Tris-(2-maleimidoethyl)amine, is altered by ATP hydrolysis: Evidence for rotation of a transmembrane helix. *J Biol Chem* **276**:31800–31805.
- Loo TW and Clarke DM (2001b) Defining the drug-binding site in the human multidrug resistance P-glycoprotein using a methanethiosulfonate analog of verapamil, MTS-verapamil. *J Biol Chem* **276**:14972–14979.
- Ma JF, Grant G, and Melera PW (1997) Mutations in the sixth transmembrane domain of P-glycoprotein that alter the pattern of cross-resistance also alter sensitivity to cyclosporin A reversal. *Mol Pharmacol* **51**:922–930.
- Prasad R, De Wergifosse P, Goffeau A, and Balzi E (1995) Molecular cloning and characterization of a novel gene of *Candida albicans*, CDR1, conferring multiple resistance to drugs and antifungals. *Curr Genet* **27**:320–329.
- Rosenberg MF, Velarde G, Ford RC, Martin C, Berridge G, Kerr ID, Callaghan R, Schmidlin A, Wooding C, Linton KJ, et al. (2001) Repacking of the transmembrane domains of P-glycoprotein during the transport ATPase cycle. *EMBO (Eur Mol Biol Organ) J* **20**:5615–5625.
- Safa AR (1998) Photoaffinity labels for characterizing drug interaction sites of P-glycoprotein. *Methods Enzymol* **292**:289–307.
- Sanglard D, Ischer F, Monod M, and Bille J (1997) Cloning of *Candida albicans* genes conferring resistance to azole antifungal agents—characterization of CDR2, a new multidrug ABC transporter gene. *Microbiol* **143**:405–416.
- Schmid D, Ecker G, Kopp S, Hitzler M, and Chiba P (1999) Structure-activity relationship studies of propafenone analogs based on P-glycoprotein ATPase activity measurements. *Biochem Pharmacol* **58**:1447–1456.
- Seelig A and Landwojtowicz E (2000) Structure-activity relationship of P-glycoprotein substrates and modifiers. *Eur J Pharm Sci* **12**:31–40.
- Senior AE, al-Shawi MK, and Urbatsch IL (1998) ATPase activity of Chinese hamster P-glycoprotein. *Methods Enzymol* **292**:514–523.
- Shani N, Sapag A, and Valle D (1996) Characterization and analysis of conserved motifs in a peroxisomal ATP-binding cassette transporter. *J Biol Chem* **271**:8725–8730.
- Servos J, Haase E, and Brendel M (1993) Gene SNQ2 of *Saccharomyces cerevisiae*, which confers resistance to 4-nitroquinoline-N-oxide and other chemicals, encodes a 169 kDa protein homologous to ATP-dependent permeases. *Mol Gen Genet* **236**:214–218.
- Shevchenko A, Wilm M, Vorm O, and Mann M (1996) Mass spectrometric sequencing of proteins from silver-stained polyacrylamide gels. *Anal Chem* **68**:850–858.
- Tmej C, Chiba P, Huber M, Richter E, Hitzler M, Schaper KJ and Ecker G, A (1998) combined Hansch/Free-Wilson approach as predictive tool in QSAR studies on propafenone-type modulators of multidrug resistance. *Arch Pharm (Weinheim)* **331**:233–240.
- van Veen HW, Venema K, Bolhuis H, Oussenko I, Kok J, Poolman B, Driessen AJM, and Konings WN (1996) Multidrug resistance mediated by a bacterial homolog of the human multidrug resistance transporter MDR1. *Proc Natl Acad Sci USA* **93**:10668–10672.
- Wiese M and Pajeva IK (2001) Structure-activity relationships of multidrug resistance reversers. *Curr Med Chem* **8**:685–713.

Address correspondence to: Dr. Peter Chiba, Institute of Medical Chemistry, University of Vienna, Waehringerstrasse 10, A- 1090 Vienna, Austria. E-mail: peter.chiba@univie.ac.at